JOURNAL OF THEORETICAL
AND APPLIED MECHANICS
4, **37**, 1999

INVESTIGATION INTO THE GROWTH DIRECTIONS OF A DUCTILE CRACK UNDER TENSILE LOADING

JIA LI

XIAO-BING ZHANG

NAMAN RECHO

LERMES, Blaise Pascal University of Clermont-Ferrand, Montluçon, France
e-mail: recho@cicsun.univ-bpclermont.fr

In this paper, we use an energy variational method to study the full stress field near a stationary crack in a plane strain state in a power-law hardening material under mode I loading. Associated with the finite element method, the trajectory line fields of the principal stresses and the maximum shear stresses have been drawn in order to determine the crack growth direction. It appears that the crack can propagate along a *cleavage band* or along a *slip band* according to the triaxial tensile stress level in the vicinity of the crack. The growth direction of a ductile crack depends on the competition between the stress concentrations along these bands.

Key words: fracture, full elastic-plastic field, crack propagation criteria

1. Introduction

The ductile fracture initiation under mode I loads can take place in tension or shear mode. When the fracture occurs in tension mode, the crack grows straight ahead of the crack tip and the crack lips open. On the other hand, for the fracture in shear mode, the crack propagate at a certain angle to the crack plane, one part of the structure slips with respect to the other. It is known that the fracture essentially relates to the void growth near the crack tip. The slip fracture depends maining on the plasticity propagation. Both the modes of fracture depend strongly on the triaxial tensile stress level existing in the vicinity of the crack tip. High triaxiality (it means that tensile stress

components are dominating) is favorable to void growth, while low triaxiality is favorable to plasticity progression.

A lot of studies have been carried out to predict fractures in tension mode in ductile materials. Hutchinson (1968) and Rice and Rosengren (1968) found out an asymptotic solution for cracks in work hardening materials (the HRR solution) which provided a theoretical foundation for the elastic-plastic fracture mechanics. According to this solution, the asymptotic stress field near the crack tip can be characterized by a single parameter, the J-integral (Rice, 1967). Basing on this solution, O'Down and Shih (1991) proposed a two-parameter theory, the $J-Q$ theory, to predict the tension fracture for engineering applications, where Q is a stress triaxiality parameter. Other models based on the development of higher-order asymptotic fields (LI and Wang, 1986; Xia et al., 1993; Yang et al., 1993) also revealed accuracy and efficiency to predict the tension fractures. However, these models may not be very adequate to predict the fractures in shear mode due to their asymptotic property. In fact, the plastic zone extends over a rather large domain around the crack tip before a slip fracture develops. Consequently, only a complete elastic-plastic solution allows for such a modeling.

Although some complete solutions for mode III cracks were obtained (Hult and McClintoc, 1957; Rice, 1967), no satisfactory solution has been found so far for mode I and mode II cracks in an elastic-plastic solid other than the Dugdale model of cracks in thin foils (Dugdale,1960). However, a few numerical approaches have been developed by several authors. Edmunds and Willis (1976a,b), (1977) developed a matching asymptotic expansion method to study the full elastic-plastic stress fields for mode III and mode I cracks in elastic-plastic materials. Another approach was that of Li (1997) who proposed an energy variational method to study the full stress field of a mode I crack for plane strain under small-scale yielding conditions. The algebraic representation of the full stress field can be obtained the near-tip plastic field, described by the HRR solution, to the far elastic one, described by the first term of Williams's expansion (Williams, 1957). Comparison with the results of finite element solutions showed that this method is highly accurate in the whole region under consideration, either for the near-tip field or for the far field.

In this paper, the variational method proposed by Li (1997) is modified by combining it with the Finite Element Method (FEM) to obtain the full stress field around the crack tip in real engineering structures. By using the complete stress solution, the trajectory fields of the principal stresses and maximum shear stresses are drawn around the crack tip. These trajectory fields clearly indicate the possible growth directions of a ductile crack. It must propagate

along a *cleavage band* if it grows in tension mode, or along a *slip band* if it grows in shear mode. The crack growth finally depends on the competition between the stress concentrations along the two directions. Basing on the fracture criteria of Ritchie et al. (1973), the prediction of the crack growth is discussed.

2. Computation procedure

2.1. Description of the method

The energy variational method proposed by Li (1997) is adapted in this work to study the full elastic-plastic stress field of a mode I crack. The main idea of this method is to establish a statically admissible stress field around the crack tip (inner field) connected to the far stress field (outer field) with the condition of stress continuously. The unknown parameters can be adjusted by minimizing the complementary energy of the structure.

Consider a material which deforms according to the Ramberg-Osgood stress-strain relationship

$$\varepsilon_{ij} = \frac{1+\nu}{E} s_{ij} + \frac{1-2\nu}{3E} \sigma_{kk} s_{ij} + \frac{3\alpha}{2E} \left(\frac{\sigma_e}{\sigma_0}\right)^{n-1} s_{ij} \tag{2.1}$$

where

- ε_{ij} – strain components
- s_{ij} – deviatoric stress components
- σ_{kk} – hydrostatic stress
- E – elastic modulus
- ν – Poisson ratio
- δ_{ij} – Kronecker delta
- α – material constant
- n – hardening exponent
- σ_0 – yielding stress
- σ_e – Mises equivalent effective stress defined as follows

$$\sigma_e = \sqrt{\frac{3}{2} s_{ij} s_{ij}} \tag{2.2}$$

The inner stress field around the crack tip is derived from a four-term expansion of the stress function ϕ_{in}

$$\phi_{in} = r^{s0}\tilde{\phi}_0(\theta) + r^{s1}\tilde{\phi}_1(\theta) + r^{s2}\tilde{\phi}_2(\theta) + r^{s3}\tilde{\phi}_3(\theta) \tag{2.3}$$

where r and θ are the polar coordinates when the origin at the crack-tip; $\widetilde{\phi}_i$, $i = 0, 1, 2, 3$ are angle-dependent functions and s_i unknown exponents with $s_0 < s_1 < s_2 < s_3$. The first term of Eq (2.3) represent the asymptotic field of the HRR solution. The last three terms can be determined using the variational technique.

The stress components of the inner field can easily be derived from Eq (2.3) as follows

$$\begin{aligned} \sigma_{rr} &= \frac{1}{r}\frac{\partial \phi_{in}}{\partial r} + \frac{1}{r^2}\frac{\partial^2 \phi_{in}}{\partial \theta^2} \\ \sigma_{\theta\theta} &= \frac{\partial^2 \phi_{in}}{\partial r^2} \\ \sigma_{r\theta} &= -\frac{\partial}{\partial r}\left(\frac{1}{r}\frac{\partial \phi_{in}}{\partial \theta}\right) \end{aligned} \tag{2.4}$$

For more convenience, we suppose that $\widetilde{\phi}_i$, can be represented by using a series of basic functions, such as polynomial functions or trigonometric functions. In this work, we expand them into the Fourier series of order q

$$\phi_i(\theta) = \sum_{j=0}^{q} a_{ij} \cos(j\theta) \qquad i = 0, 1, 2, 3 \tag{2.5}$$

Then Eq (2.3) can be rewritten as follows

$$\phi_{in} = r^{s_0} \sum_{j=0}^{q} a_{0j} \cos(j\theta) + \sum_{i=1}^{3} r^{s_i} \sum_{j=0}^{q} a_{ij} \cos(j\theta) \tag{2.6}$$

Only the cosine functions are taken into account in the Fourier series due to the symmetry of the mode I problem. The coefficients a_{0j} can be calculated by developing the HRR solution into the Fourier series, while the coefficients a_{ij} $(i > 0)$ can be determined by considering the continuity between the inner and outer fields.

Suppose that the outer field is already known by its stress function ϕ_{out}. Similarly to Eq (2.5), ϕ_{out} and its partial derivatives with respect to r at the circle boundary $r = R$ can also be developed into the Fourier series of order q

$$\begin{aligned}
&\phi_{out}(r=R)=\sum_{j=0}^{q} b_{0j}\cos(j\theta)\\
&\frac{\partial\phi_{out}}{\partial r}(r=R)=\sum_{j=0}^{q} b_{1j}\cos(j\theta)\\
&\frac{\partial^2\phi_{out}}{\partial r^2}(r=R)=\sum_{j=0}^{q} b_{2j}\cos(j\theta)\\
&\ldots
\end{aligned}\tag{2.7}$$

The inner field and the outer field must be connected continuously across the circle boundary $r=R$. According to Eqs (2.4), the minimum order of the continuity between the two stress functions is C^2 to ensure the continuity of all stress components. It is easy to demonstrate that these continuity conditions can be readed only when the stress functions and their derivatives with respect to r are continuous across the circle boundary $r=R$, if the stress functions are expanded into the Fourier series. This condition leads to the following equations

$$\begin{aligned}
&R^{s_0}\sum_{j=0}^{q} a_{0j}\cos(j\theta)+\sum_{i=1}^{3} R^{s_i}\sum_{j=0}^{q} a_{ij}\cos(j\theta)=\sum_{j=0}^{q} b_{0j}\cos(j\theta)\\
&s_0R^{s_0-1}\sum_{j=0}^{q} a_{0j}\cos(j\theta)+\sum_{i=1}^{3} s_iR^{s_i-1}\sum_{j=0}^{q} a_{ij}\cos(j\theta)=\sum_{j=0}^{q} b_{1j}\cos(j\theta)\\
&s_0(s_0-1)R^{s_0-2}\sum_{j=0}^{q} a_{0j}\cos(j\theta)+\sum_{i=1}^{3} s_i(s_i-1)R^{s_i-2}\sum_{j=0}^{q} a_{ij}\cos(j\theta)=\\
&=\sum_{j=0}^{q} b_{2j}\cos(j\theta)
\end{aligned}\tag{2.8}$$

These equations must be true for all angles. One immediately obtains $q+1$ systems of linear equations

$$\begin{aligned}
&R^{s_1}a_{1j}+R^{s_2}a_{2j}+R^{s_3}a_{3j}=b_{0j}-R^{s0}a_{0j}\\
&s_1R^{s_1-1}a_{1j}+s_2R^{s_2-1}a_{2j}+s_3R^{s_3-1}a_{3j}=b_{1j}-s_0R^{s0-1}a_{0j}\\
&s_1(s_1-1)R^{s_1-2}a_{1j}+s_2(s_2-1)R^{s_2-2}a_{2j}+s_3(s_3-1)R^{s_3-2}a_{3j}=\\
&=b_{2j}-s_0(s_0-1)R^{s_0-2}a_{0j}
\end{aligned}\tag{2.9}$$

where $j = 0, 1, ..., q$. Then the coefficients a_{ij} can be calculated by solving these systems of linear equations. The results can be written under matrix form

$$\mathbf{A} = \mathbf{R}^{-1}\mathbf{B} \tag{2.10}$$

where

$\mathbf{A}$ – unknown constant matrix, $\mathbf{A} = [a_{ij}]$, $i = 1, 2, 3$, $j = 0, 1, ..., q$

$\mathbf{R}$ – constant matrix of dimension 3×3

$\mathbf{B}$ – constant matrix of dimension $3 \times (q + 1)$ and

$$\mathbf{R} = \begin{bmatrix} R^{s_1} & R^{s_2} & R^{s_3} \\ s_1 R^{s_1-1} & s_2 R^{s_2-1} & s_3 R^{s_3-1} \\ s_1(s_1-1)R^{s_1-2} & s_2(s_2-1)R^{s_2-2} & s_3(s_3-1)R^{s_3-2} \end{bmatrix} \tag{2.11}$$

$$\mathbf{B} = \begin{bmatrix} b_{00} - R^{s_0}a_{00} & b_{01} - R^{s_0}a_{01} & \dots \\ b_{10} - s_0 R^{s_0-1}a_{00} & b_{11} - s_0 R^{s_0-1}a_{01} & \dots \\ b_{20} - s_0(s_0-1)R^{s_0-2}a_{00} & b_{21} - s_0(s_0-1)R^{s_0-2}a_{01} & \dots \end{bmatrix}$$

From Eqs (2.10) and (2.11), all unknown constants a_{ij} can be obtained by a simple matrix multiplication.

To determine the 3 exponents s_1, s_2 and s_3, the theorem of minimum complementary energy is used. The complementary energy U_c of a structure which obeys the stress-strain relationship defined by Eq (2.1) for either plane stress or plane strain is

$$U_c = \int_{\Omega} \left[\frac{1+\nu}{3E}\sigma_e^2 + \frac{1-2\nu}{6E}\sigma_{kk}^2 + \frac{\alpha\sigma_0^2}{E(n+1)}\left(\frac{\sigma_e}{\sigma_0}\right)^{n+1} \right] d\Omega \tag{2.12}$$

The integration is performed over the circle area Ω, $r < R$.

The problem then consists in finding out the parameters (s_1, s_2, s_3) so that the complementary energy becomes stationary and minimum. This minimization problem can be solved by using numerical methods.

By substituting (s_1, s_2, s_3) into Eq (2.10), all coefficients a_{ij} can be determined. The stress function of the inner field is completely defined by Eq (2.6). The stress components can therefore be derived from Eqs (2.4).

2.2. Numerical procedures

The plane-strain crack-tip stress field is determined by using the method described in section 2.1 associated with the FEM. The far stress field at the

circle boundary $r = R$ is given by the finite-element modeling which does not need to be very fine. The finite-element modeling also allows us to verify the accuracy of the energy variational method in the elastic-plastic zone near the crack tip.

In general, the finite-element analysis yields only the stress components at the circle boundary. From these stress components, the stress function and its derivatives with respect to r can be solved according to Eqs (2.4)

$$\begin{aligned}
&\phi_{out}(R,\theta) = R^2\Big[\sin\theta\Big(\int_0^\theta - \int_0^\pi\Big) f(\theta)\cos\theta\, d\theta - \cos\theta\Big(\int_0^\theta - \int_0^\pi\Big) f(\theta)\sin\theta\, d\theta\Big] \\
&\frac{\partial\phi_{out}(R,\theta)}{\partial r} = \frac{\phi_{out}(R,\theta)}{R} - R\int_0^\theta \sigma_{r\theta}(R,\theta)\, d\theta \qquad (2.13) \\
&\frac{\partial^2\phi_{out}(R,\theta)}{\partial r^2} = \sigma_{\theta\theta}(R,\theta)
\end{aligned}$$

where

$$f(R,\theta) = \sigma_{rr}(R,\theta) + \int_0^\theta \sigma_{r\theta}(R,\theta)\, d\theta$$

The integration can be performed by using a numerical method. Knowing the stress distribution at the circle boundary $r = R$, the stress function and its derivatives of the outer field with respect to r can be obtained from Eqs (2.13).

By using the energy variational method and the boundary conditions (2.13), we carry out detailed computations of the stress fields for a Single Edge Cracked Panel (SECP) with the three a/w ratios: 0.1, 0.5, and 0.9, where a is the crack length and w the specimen width. When the crack is short, the uncracked ligament is mainly subjected to tension; while the uncracked ligament is mainly subjected to bending when the crack becomes longer. So the triaxiality near the crack tip varies with the crack length.

The geometry of the specimen and the finite element mesh are illustrated in Fig.1. Different loading levels are chosen such that the plastic deformations develop from small-scale yielding to full yielding. The values of the material properties used in the calculations are $n = 10$, $E/\sigma_0 = 300$, $\nu = 0.3$ and $\alpha = 1$. A general-purpose FEM program, CASTEM 2000, is used for preliminary computations.

The outer field, represented by the stress distribution at the circle boundary $r = R$, is evaluated using the FEM. These stress components are converted into the stress function and its derivatives by using Eqs (2.13). The

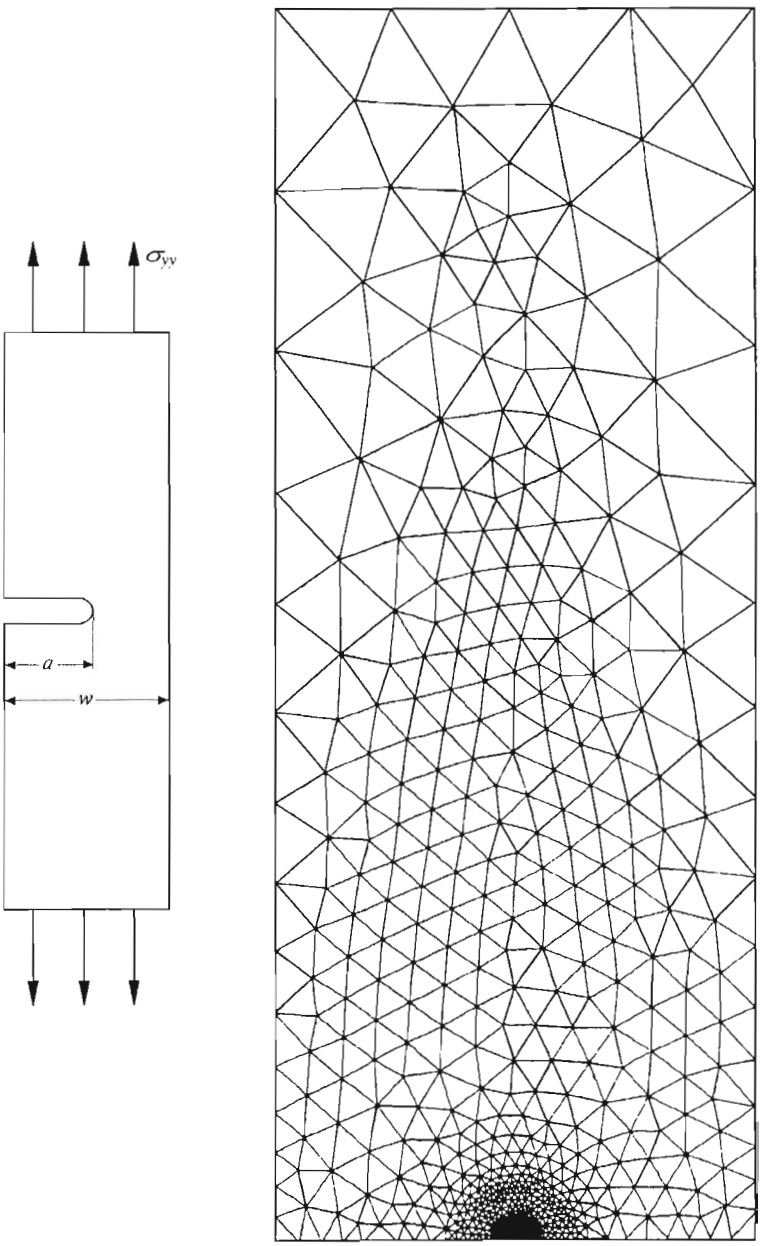

Fig. 1. Geometry and finite element mesh of the specimens

choice of the radius R does not influence much the calculation accuracy. However, this radius cannot be too long because the inner field is approached only by a four-term expansion. In this work, $R = 0.05w$ is chosen for specimens with short cracks, while $R = 0.09w$ is chosen for specimens for long cracks.

The near-tip asymptotic field, described by the first term of expansion (2.5), is characterized by the J-integral which can be determined in the finite element modeling. The virtual crack extension method developed by Parks (1974), implemented into the CASTEM 2000 program, is used to calculate the J-integral. Knowing the value of the J-integral, the amplitude of the HRR solution can be determined.

Then the first terms of the inner field and the outer field, respectively, are expanded into the Fourier series as described in Eqs (2.6) and (2.7). Thus all the coefficients in the stress function of the inner field can be obtained by a simple matrix multiplication (se Eq (2.10)).

The different exponents s_1, s_2, s_3 can be calculated by minimizing the complementary energy in the structure. The numerical procedure used in this work is the downhill simplex method. This method is easy to use to find out the minimum of a function of more than one independent variable. With this method, the exponent vector $[s_1, s_2, s_3]$ can be found. The convergence is ensured by this method for any initial simplex guessed . However, a local minimum point may be reached. So it is preferable to proceed to several downhills with different initial simplexes. The optimal point can be chosen after survey of the results.

3. Results and discussions

3.1. Complete stress fields around the crack tip

The power exponents in Eq (2.3) obtained for SECPs with different crack lengths and loading levels are listed in Table 1. Table 1 shows that in all cases studied in this work, a 4-term expansion (including the HRR solution) is sufficient to connect accurately the inner elastic-plastic stress field near the crack tip to the far outer field. The exponent of the last term is often very big. This means that its influence on the near tip stress distribution is very small, nearly negligible. It is also seen that the inner field extends largely over distances of $5J/\sigma_0$ encompassing length scales in the tension fracture process zone, both in small- and large-scale yieldings.

Table 1: Power exponents in the expansions of the complete solution

a/w	R/w	J [N/mm]	yielding scale	s_0	s_1	s_2	s_3
0.1	0.05	2.77	SSY	1.909	2.65	2.74	30
0.1	0.05	15.99	MSY	1.909	2.03	2.96	85
0.1	0.05	63.93	LSY	1.909	2.00	2.85	200
0.5	0.05	3.17	SSY	1.909	2.58	2.69	9.46
0.5	0.05	13.82	MSY	1.909	2.30	2.48	250
0.5	0.05	72.29	FY	1.909	2.15	5.35	128
0.9	0.09	2.77	SSY	1.909	2.65	2.74	28
0.9	0.09	15.99	MSY	1.909	3.60	3.65	3.70
0.9	0.09	30.16	FY	1.909	3.42	3.45	3.51

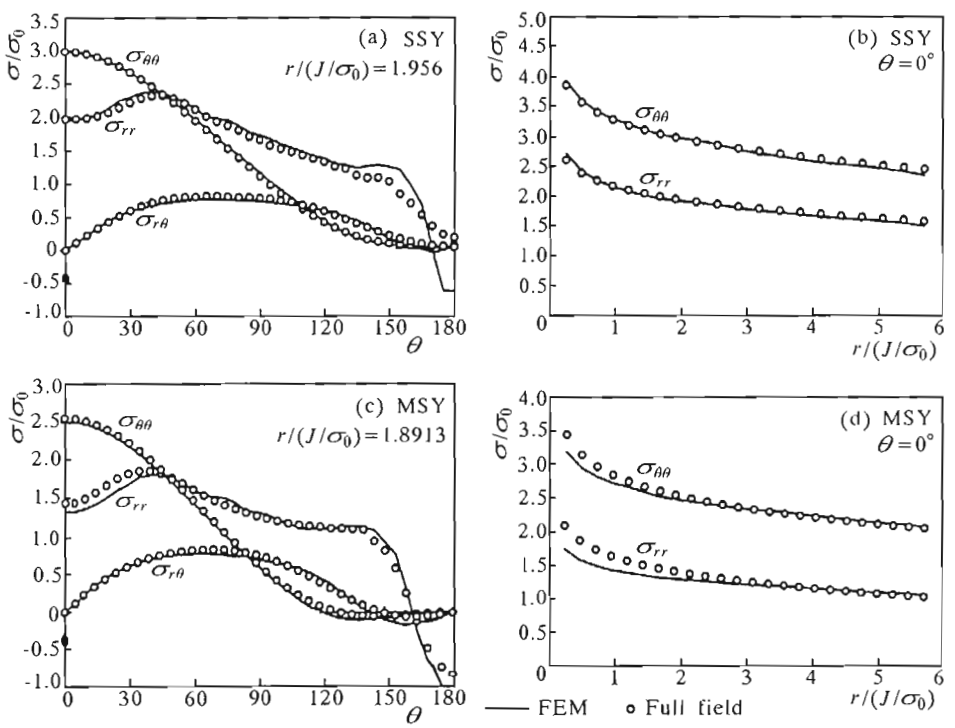

Fig. 2. Comparison of the stress fields between the results of the finite element modeling and of the complete solution for $a/w = 0.1$; (a), (c) – angular distribution of the stress components, (b), (d) – radial distribution of the stress components ahead of the crack

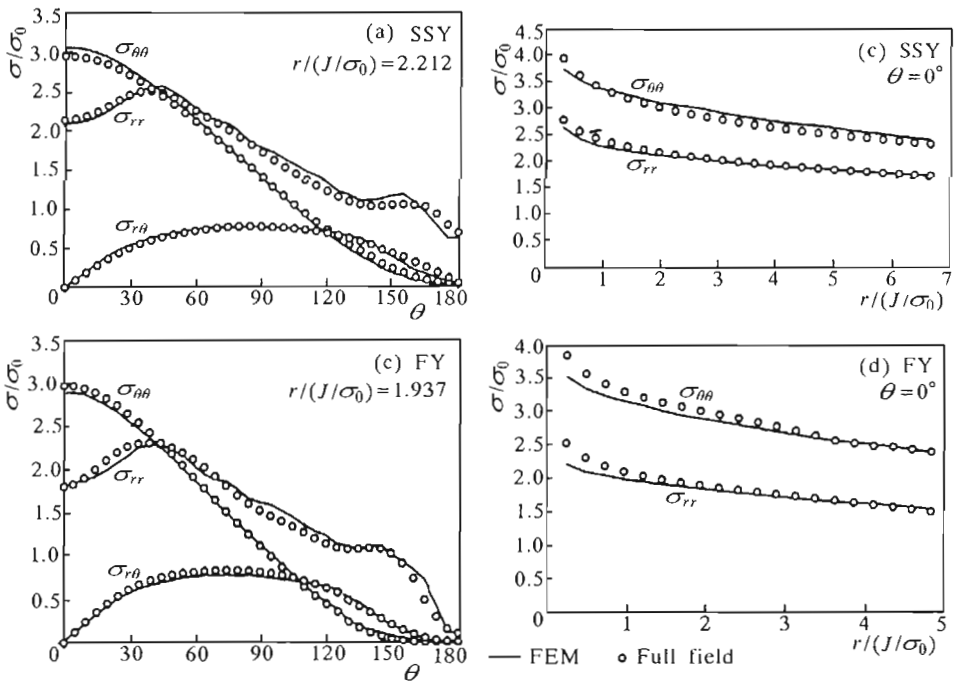

Fig. 3. Comparison of the stress fields between the results of the finite element modeling and of the complete solution for $a/w = 0.5$; (a), (c) – angular distribution of the stress components, (b), (d) – radial distribution of the stress components ahead of the crack

In order to verify the results of this approach, we compare the complete solutions with those of the FEM. The results of such comparisons are presented in Fig.2 ÷ Fig.4. The angular distributions of the stress components are illustrated for distances $r \cong 2J/\sigma_0$ from the crack tip, while the radial distributions are presented along the uncracked ligament near the crack tip within distances $r < 10J/\sigma_0$. Fig.2 ÷ Fig.4 show a total agreement between the complete solutions of the energy method and those of the FEM for short and long cracks under the SSY and LSY conditions. This means that a four-term expansion can accurately describe the inner stress field near the crack tip which is connected to the far field of any real engineering structure. These results confirm those obtained by Li (1997) who used the first term in pure elastic expansion as the far outer field.

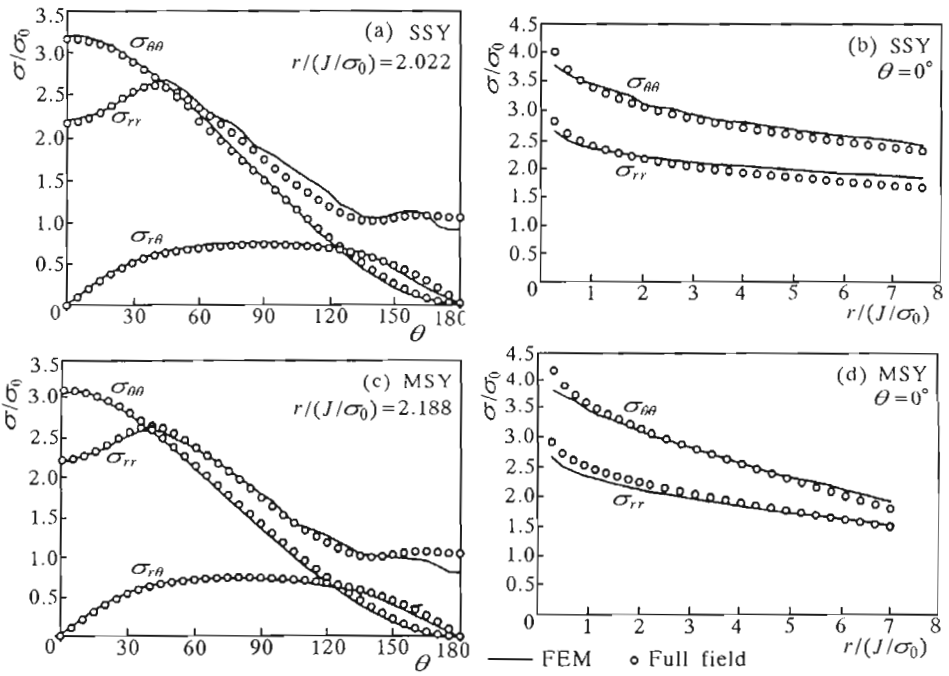

Fig. 4. Comparison of the stress fields between the results of the finite element modeling and of the complete solution for $a/w = 0.9$; (a), (c) – angular distribution of the stress components, (b), (d) – radial distribution of the stress components ahead of the crack

3.2. Fractures in tension mode

In recent studies, the criterion proposed by Ritchie et al. (1973), known as the RKR criterion, was often used to predict the tension propagation of an elastic-plastic crack. According to this criterion, the tension fracture requires achieving a critical normal stress σ_c at a critical distance r_{Ic} along a line where the normal tensile stresses are maximum. This line, if called the tension line, must be one of the trajectory lines of the principal stresses starting from the crack tip (since $\tau_{r\theta} = 0$ when $\sigma_{\theta\theta}$ is maximum according to Eqs (2.4)). In the mode I problem, the tension line is just along the uncracked ligament ahead of the crack tip. However, in the mixed mode problem, this line may not be a straight line ahead of the crack tip. In this case, the tension line can be obtained only if the complete solution is known. In this work, the possibility to obtain the tension line in the mode I problem is presented. The cases for the mixed mode will be the subject of forthcoming studies.

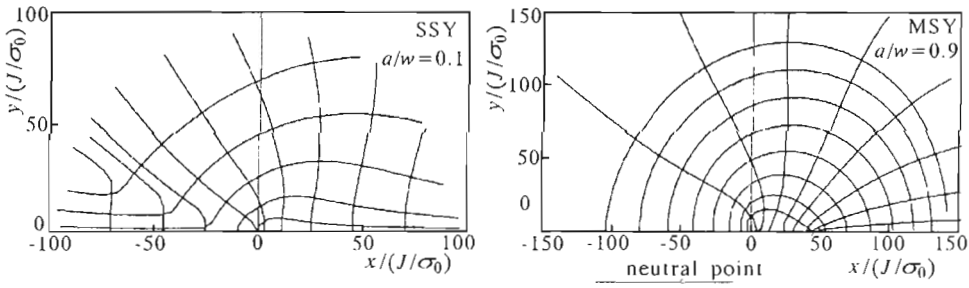

Fig. 5. Trajectory line fields of the principal stresses near the crack tip

The trajectory lines of the principal stresses for the in-plane problem are easy to obtain by using the Mohr circle technique if the stress field is known. By using the complete solution mentioned above, the trajectory lines of the principal stresses of SECP specimens are drawn both for a short crack $(a/w = 0.1)$ and a long crack $(a/w = 0.9)$ as shown in Fig.5. From Fig.5, one can see that the principal stresses near the crack tip always follow the direction of the crack plane by forming a *cleavage band.* It means that if the crack grows in tension mode, it will always follow this band. The heterogeneity of the material may perturb the growth direction on microstructural scale. However, the crack growth on macroscopic scale must be governed by the cleavage band. Fig.5 also shows that the trajectory field of the principal stresses of a short-cracked specimen are quite different from that of a long-cracked one. In a short-cracked specimen, where the uncracked ligament is essentially subjected to tension, the cleavage band stretches quite far away from the crack tip; while in a long-cracked specimen, where the uncracked ligament is essentially subjected to bending, the cleavage band stops at a neutral point beyond which the ligament is subjected to compression.

3.3. Fractures in shear mode

If the crack propagates in a ductile mode, the plasticity will progress from the crack tip until a characteristic size is reached along a maximum shear stress direction, before a fracture is observed. Few criterion studies have dealt with this type of fractures so far. However, fractures in tension mode have been observed in many experimental studies. Shih and German (1981) reported that they occurred in A533B steel center-cracked panels (CCP) under tensile loads when the cracks were deep enough. They also noted that the shear fracture toughness was almost twice as high as that of the tension fractures.

Shear fractures can be studied if one knows the complete solution of the stress field around the crack tip. In an elastic-plastic 2D structure, the plasticity develops along the planes of the maximum shear stresses. The maximum shear stress at a point can be calculated when the three principal stresses are known

$$\tau_{max} = \frac{\sigma_1 - \sigma_3}{2} \tag{3.1}$$

where σ_1 is the maximum principal stress and σ_3 is the minimum principal stress. τ_{max} makes $45°$ with σ_1 and σ_3. The growth direction of a ductile crack can be determined by drawing the trajectory lines of the maximum shear stresses near the crack tip. The complete solutions facilitate this work.

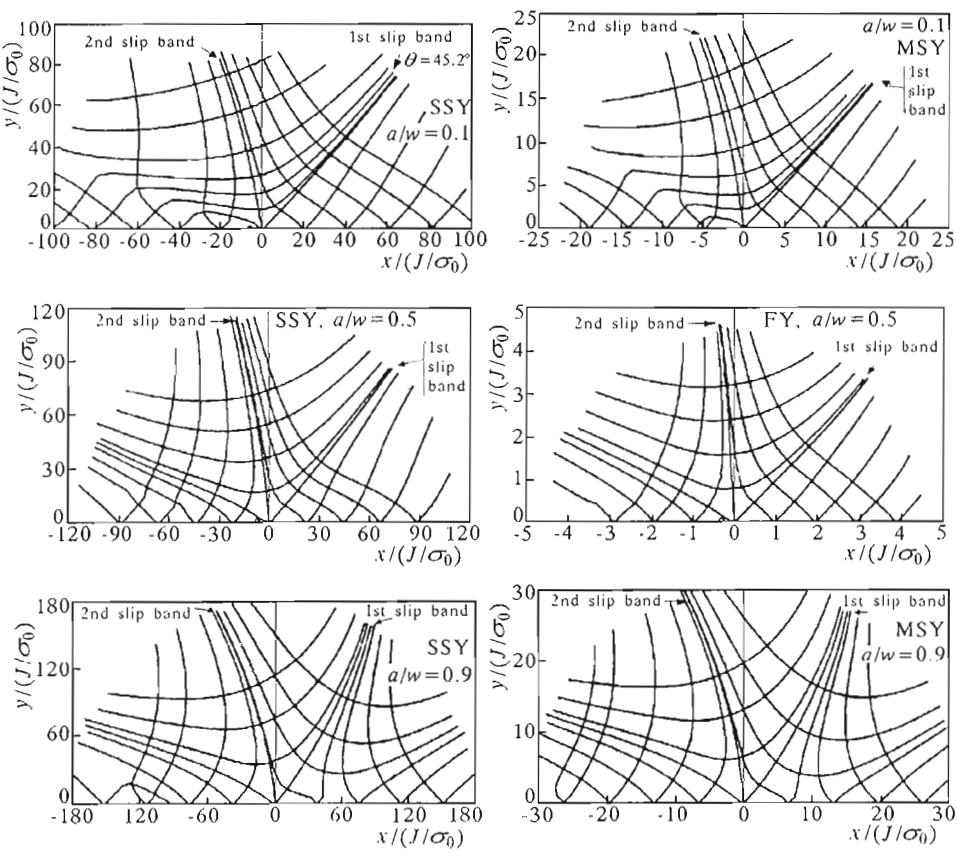

Fig. 6. Trajectory line fields of the maximum shear stresses, SECP

Fig.6 shows these trajectory line fields of SECPs for different crack lengths and loading levels. Fig.6 shows that the trajectory lines of the maximum shear

stresses concentrate in several directions from the crack tip by forming some *slip bands*. One can observe 3 slip bands for all specimen geometries considered: the first with $\theta \cong 50°$, the second with $\theta \cong 100°$ and the third with $\theta \cong 140°$. From Fig.6, it is observed that from any point situated in the vicinity of the crack tip, the trajectory lines of the maximum shear stresses will follow one of the three slip bands. It means that if the plasticity develops in the vicinity of the crack tip, it will progress in one of these directions and will cause the structure to slip in the XY-plane.

From Fig.6, one can clearly observe the difference between the direction of the first slip band of a short-cracked SECP and that of a deeply-cracked one. The first slip band in the short-cracked SECP makes about $45°$ with the crack plane. This angle is bigger when the crack becomes longer. It can reach $65°$ for a deeply-cracked SECP. This phenomena show that the slip mode for a crack subjected to dominating tension is quite different from that for a crack subjected to dominating bending.

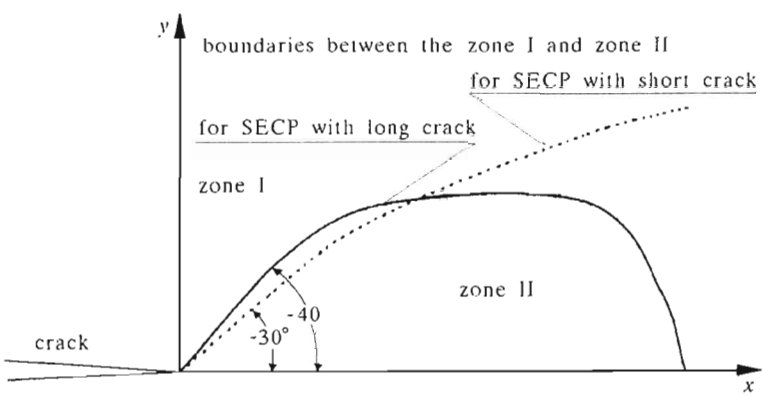

Fig. 7. Division of the region near the crack tip into zone I and zone II

Calculations show that the maximum shear stresses along the third slip band are smaller than those along the first two ones. Therefore one can conclude that there is little probability for the crack to grow in this direction. However, the magnitude of the maximum shear stresses along the first slip band is comparable to that along the second one. Fig.7 shows the maximum shear stresses along these two slip bands in a short cracked specimen and in a long-cracked one. From Fig.8, one can observe that the maximum shear stresses along the second slip band are higher than those along the first within a certain distance from the crack tip, and beyond it become lower. The maximum shear stresses rapidly decrease along the second slip band. The plasticity

is limited by the geometry of the specimen and does not develop sufficiently. This may explain why few slip fractures in this direction have been observed in experimental studies. On the other hand, the maximum stresses along the first slip band are higher than those along the second one for long distances. Therefore, the plasticity will develop essentially along this direction. One can conclude that the slip fracture will essentially occur along the first slip band under mode I loading.

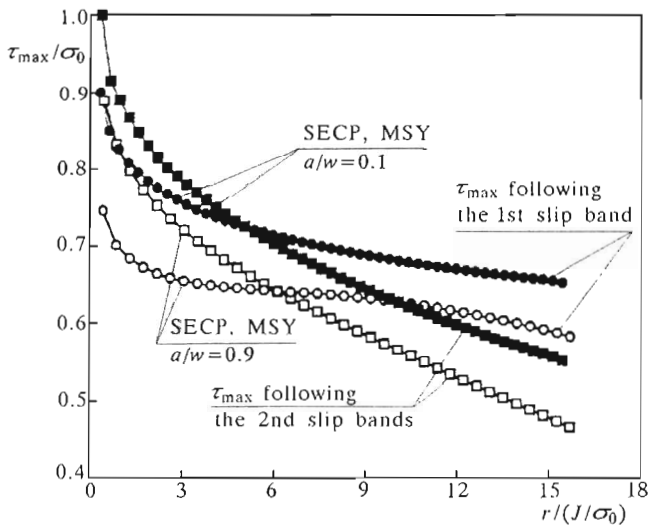

Fig. 8. Maximum shear stresses along the first two slip bands for $a/w = 0.1$ and 0.9

It is also important to note that the maximum shear stresses along the two slip bands in short-cracked SECPs are higher than those in deeply-cracked SECPs. This explains why the slip fractures are often found in specimens whose uncracked ligaments are subjected to dominating tension.

These remarks do agree with the experimental results. The experimental studies of Shih and German (1981) into the deeply-cracked CCPs of A533B steels showed that slip fracture occurred in the direction of about 45° with the crack plane. The analysis of the slip bands of the full stress field in this work predicts exactly the same direction for low- hardening plastic materials.

Remark: In the case of plane strain under tensile loads, the maximum principal stress σ_1 is always in the structure plane, i.e. in the XY-plane. However, the minimum principal stress σ_3 may be in the XY-plane or in the direction perpendicular to it, i.e. along the Z-axis. According to σ_3 situated in the XY-plane or along the Z-axis, the region near the crack tip can be

divided into several different zones. In the zones belonging to the first case, say zones I, the maximum shear stress τ_{max} is in the XY-plane too. In the zones belonging to the second case, say zones II, τ_{max} makes $45°$ with the XY-plane. Fig.7 shows the division of the region near the crack tip into such zones for SECPs according to our calculations. For shorter cracks, zone II is an open area and limited by $|\sigma| < 30°$. For longer cracks, this zone is a closed area and bounded by $|\sigma| < 40°$ near the crack tip. From Fig.6, one can notice that all the three slip bands are located in zone I. This means that in plane strain, the plasticity develops mainly in the XY-plane. However, in real 3D structures, the crack may propagate by slip at $45°$ with the XY-plane in zone II close to the specimen surface where the plane stress dominates. In this study, this situation is not considered.

3.4. Competition between tension and shear fractures

The analysis of the trajectory line fields of the principal stresses and of the maximum shear stresses enables us to determine the cleavage bands and the slip bands of cracked structures. Possible directions of the crack initiation can be estimated by this analysis. But such an analysis can not predict in which direction the crack will grow. To answer this question, these two modes of fractures must be put into competition. However, few satisfactory criteria considering this competition have been proposed in the literature.

In this paper, we try to show that this competition exists near the crack tip in structures under tensile loading and considering this competition may be an efficient method for the prediction of the crack propagation.

As an example, we simulate such a competition for SECPs under different loading levels. According to the discussion in Section 3.3, only the slip fracture following the first slip band is taken into account. In order to show the trend of the crack growth, the tension stresses σ at the cleavage band and the shear stress τ at the slip band are calculated for different crack lengths. σ is calculated at distance $r = 0.05$ from the crack tip, and τ is calculated at distance $r = 0.5$ from the crack tip. Using different values of distance r near the crack tip leads to similar behaviours. The results are represented against the value of the J-integral as shown in Fig.9. From Fig.9, it is observed that when the loading level is low, the values of $\sigma(r = 0.05)$ are nearly identical for all initial crack lengths. As the loading level increases, the values of $\sigma(r = 0.05)$ increase at different rates for differently-cracked specimens. In the specimen with $a/w = 0.9$, $\sigma(r = 0.05)$ increases more rapidly than in the other two specimens ($a/w = 0.5$ and 0.1). It is when $a/w = 0.1$ that $\sigma(r = 0.05)$

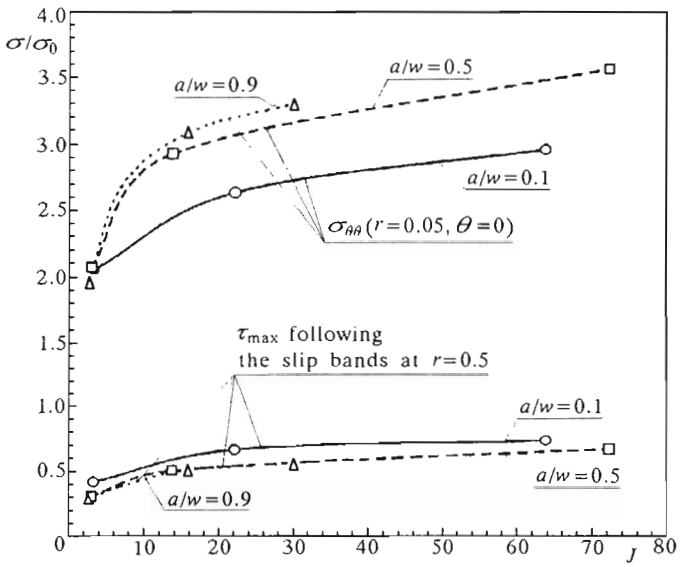

Fig. 9. Competition between the characteristic stresses $\sigma(r = 0.05)$ and τ $(r = 0.5)$ in SECP specimens

increases most slowly. It means that the triaxial tension level in the vicinity of the crack tip increases more rapidly in bending-loaded specimens than in tension-loaded ones as the remote loads increase. The opposite phenomenon is observed for the values of $\tau(r = 0.5)$. In this case, the maximum shear stress $\tau(r = 0.5)$ is higher in the short-cracked SECP $(a/w = 0.1)$ than in the deeply-cracked ones $(a/w = 0.5$ and $0.9)$. Therefore one can conclude that in bending-loaded specimens, the tension fractures are more probable. On the other hand, in tension-loaded specimens, the slip fractures are more probable.

This example shows the necessity for including the competition between fractures in tension mode and in shear mode in the criteria of the crack initiation. Establishment of such criteria will have to be carried out in further experimental studies.

4. Conclusion

An energy variational method has been proposed to study the complete solution of the stress field near a stationary, plane strain, mode I crack in a power-law hardening material. In association with the FEM, this analysis

can be used in real engineering structures. It is shown that in general, a four-term expansion of the stress function is sufficient to describe the stress field accurately, both near and far from the crack tip. This property allows us to examine the plasticity development which can extend over a large region before a slip fracture occurs. By using the Mohr circle technique, the trajectory fields of the principal stresses and the maximum shear stresses have been drawn from the complete solution in order to determine the crack growth direction. One notices that the crack can propagate along a *cleavage band* or along a *slip band* according to the triaxial tensile stress level in the vicinity of the crack. These bands can easily be found from the trajectory fields. The growth direction of a ductile crack finally depends on the competition of the stress concentrations along these bands.

References

1. DUGDALE D.S., 1960, Yielding of Steel Sheets Containing Slits, *J. Mech. Phys. Solids*, **8**, 100-104
2. EDMUNDS T.M., WILLIS J.R., 1975a, Matched Asymptotic Expansions in Non-Linear Fracture Mechanics – I. Longitudinal Shear of an Elastic Perfectly-Plastic Specimen, *J. Mech. Phys. Solids*, **24**, 205-223
3. EDMUNDS T.M., WILLIS J.R., 1975b, Matched Asymptotic Expansions in Non-Linear Fracture Mechanics – II. Longitudinal Shear of an Elastic Work-Hardening Plastic Specimen, *J. Mech. Phys. Solids*, **24**, 225-237
4. EDMUNDS T.M., WILLIS J.R., 1977, Matched Asymptotic Expansions in Non-Linear Fracture Mechanics – III. In-Plan Loading of an Elastic Perfectly-Plastic Symmetric Specimen, *J. Mech. Phys. Solids*, **25**, 423-455
5. HULT J.A., MCCLINTOC, 1957, Elastic-Plastic Stress and Strain Distribution Around Sharp Notches under Repeated Shear, *Proc. 9th Int. Cong. Appl. Mech.*, **8**, 51-62
6. HUTCHINSON J.W., 1968, Singular Behavior at the End of a Tensile Crack in a Hardening Material, *J. Mech. Phys. Solids*, **16**, 13-31
7. LI J., 1997, Determination of the Full Elastic-Plastic Stress Field of a Tensile Crack by Minimization of the Complementary Energy, *Int. J. Fracture*, **84**, 1-17
8. LI Y., WANG Z., 1986, High-Order Asymptotic Field of Tensile Plane-Strain Non-Linear Crack Problems, *Scientia Sinica*, **A9**, 941-955
9. O'DOWN N.P., SHIH C.F., 1991, Family of Crack-Tip Fields Characterized by a triaxiality Parameter – I. Structure of Fields, *J. Mech. Phys. Solids*, **39**, 989-1015

10. PARKS D.M., 1974, A Stiffness Derivative Finite Element Technique for Determination of Crack Tip Stress Intensity Factors, *Int. J. Fracture*, **10**, 487-501

11. RICE J.R., 1967, Stresses Due to a Sharp; Notch in a Work-Hardening Elastic-Plastic Material Loaded by Longitudinal Shear, *J. Appl. Mech.*, **34**, 287-298

12. RICE J.R., 1968, A Path Independent Integral and the Approximate Analysis of Strain Concentrations by Notches and Cracks, *J. Appl. Mech.*, **35**, 379-386

13. RICE J.R., ROSENGREN G.F., 1968, Plane Strain Deformation Near a Crack Tip in a Power-Law Hardening Material, *J. Mech. Phys. Solids*, **16**, 1-12

14. RITCHIE R.O, KNOTT J.F., RICE J.R., 1973, *J. Mech. Phys. Solids*, **21**, 395

15. SHIH C.F., GERMAN M.D., 1981, Requirement for a one Parameter Characterization of Crack Tip Field by the HRR Singularity, *Int. J. Fracture*, **17**, 27-43

16. WILLIAMS M.L., 1957, On the Stress Distribution at the Base of a Stationary Crack, *J. Appl. Mech.*, **24**, 111-114

17. XIA L., WANG T.C., SHIH C.F., 1993, Higher-Order Analysis of Crack Tip Fields in Elastic Power-Law Hardening Materials, *J. Mech. Phys. Solids*, **41**, 665-687

18. YANG S., CHAO Y.J., SUTTON M.A., 1993, Higher Order Asymptotic Crack Tip Fields in a Power-Law Hardening Material, *Eng. Fracture Mech.*, **45**, 1-20

Badania kierunków wzrostu pęknięcia ciągliwego przy obciążeniu rozciągającym

Streszczenie

W pracy zastosowano metodę wariacji energii do badania pełnego pola naprężeń wokół stacjonarnego pęknięcia w płaski stanie odkształcenia dla materiału o potęgowym wzmocnieniu dla I typu obciążenia. Przy pomocy metody elementów skończonych wyznaczono pola trajektorii naprężeń głównych i maksymalnych naprężeń ścinających w celu określenia kierunku wzrostu szczeliny. Stwierdzono, że pęknięcie rozwija się wzdłuż pasm rozdzielczości lub pasm ścinania, zgodnie z poziomem trójosiowych naprężeń rozciągających w otoczeniu pęknięcia. Kierunek wzrostu pęknięcia ciągliwego zależy od relacji pomiędzy koncentracjami naprężeń wzdłuż tych pasm.

Manuscript received June 17, 1998; accepted for print November 23, 1998